Open access • Journal Article • DOI:10.1063/1.1596553

Evidence from human scalp electroencephalograms of global chaotic itinerancy

Walter J. Freeman

Institutions: University of California, Berkeley

Published on: 22 Aug 2003 - Chaos (AIP Publishing)

Title
Evidence from human scalp electroencephalograms of global chaotic itinerancy

Journal
Chaos, 13(3)

ISSN
1054-1500

Author
Freeman, Walter J, III

Publication Date
2003-09-01

Peer reviewed

Evidence from human scalp EEG of global chaotic itinerancy

Walter J. Freeman
Department of Molecular and Cell Biology, University of California, Berkeley, California 94720-3200

(Received 28 January 2003; accepted 10 June 2003)

My objective of this study was to find evidence of chaotic itinerancy in human brains by means of noninvasive recording of the EEG from the scalp of normal subjects. My premise was that chaotic itinerancy occurs in sequences of cortical states marked by state transitions that appear as temporal discontinuities in neural activity patterns. I based my study on unprecedented advances in spatial and temporal resolution of the phase of oscillations in scalp EEG. The spatial resolution was enhanced by use of a high-density curvilinear array of 64 electrodes, 189 mm in length, with 3 mm spacing. The temporal resolution was advanced to the limit provided by the digitizing step, here 5 ms, by use of the Hilbert transform. The numerical derivative of the analytic phase revealed plateaus in phase that lasted on the order of 0.1 s and repeated at rates in the theta (3–7 Hz) or alpha (7–12 Hz) ranges. The plateaus were bracketed by sudden jumps in phase that usually took place within 1 to 2 digitizing steps. The jumps were commonly synchronized in each cerebral hemisphere over distances of up to 189 mm, irrespective of the orientation of the array. The jumps were usually not synchronized across the midline separating the hemisphere or across the sulcus between the frontal and parietal lobes. I believe that the widespread synchrony of the jumps in analytic phase manifest a metastable cortical state in accord with the theory of self-organized criticality. The jumps appear to be subcritical bifurcations. They reflect the aperiodic evolution of brain states through sequences of attractors that on access support the experience of remembering. © *2003 American Institute of Physics.* [DOI: 10.1063/1.1596553]

Precision measurements of human scalp EEG have repeatedly demonstrated nearly zero lag synchrony within ±1 ms of oscillatory potentials in the frequency range of 12–50 Hz at multiple sites covering distances exceeding 0.20 m. This phase locking seems inconsistent with the reliance of brains for intercortical communication on action potentials propagating at 5–10 m/s that impose distance-dependent delays often exceeding 40 ms. Recent advance in application of the Hilbert transform to scalp EEG has revealed new evidence for abrupt changes in analytic phase that occur simultaneously over multiple brain areas and repeat irregularly at mean rates of 3–12 Hz. From the 1/*f* spatial and temporal spectra of intracranial EEG it appears that the brain maintains a state of self-organized criticality (SOC) as the basis for its capacity for rapid adjustment to environmental challenges. State changes resembling phase transitions occur continually everywhere in cortex at scales ranging from mm to an entire hemisphere, and from a few ms to several hundred ms. Only the largest and longest-lasting states appear in scalp EEG, giving the appearance of chaotic itinerancy. Multiple phase measurements have revealed two classes of conduction delays that recall anomalous dispersion in optical media. Transmission of information by action potentials acting on synapses is at group velocities requiring tens of ms for completion. The spread of phase transitions is at phase velocities that are much faster, which are explained by three biological factors. First, the modal length of cortical axons is ~1 mm, but a small percentage is intercortical up to 0.2 m. These long axons mediate small world effects. Second, SOC holds the forebrain at the edge of instability, so that low local neural activity of a kind that is meaningful for the subject can trigger a massive state change. Third, the neural activity of populations is broadcast by axonal pathways that perform spatial integral transforms and that extract the spatially coherent fraction of the activity. That same fraction largely determines the scalp EEG. These new EEG phase data are presented to physicists and mathematicians in hope of enlisting them in the work of devising new brain dynamic models based in advanced physical concepts.

I. INTRODUCTION

The concept of chaotic itinerancy (Tsuda, 2001) implies that a complex system such as the human brain evolves by steps along a trajectory in state space. Each step marks the shift from one basin of attraction to another. In a closed system the next attractor would be selected solely by internal system dynamics. The brain is an open system that is engaged with its environments. It continually updates itself by sensory input from external receptors facing the world and from internal receptors gathering information about the states of the muscles, skeleton, and viscera. Owing to changes with learning, trajectories continually change. Although no two successive states are identical, preferred states form classes by abstraction and generalization, which are statistically reliable, so that trajectories have recognizable chains and loops in brain state space.

The brain states can be inferred from classes of behavior, which include repeated actions by animals and humans in the

forms of conditioned reflexes, habits, and traits that are easily recognized by observers. A class of actions that is unique to humans includes verbal reports of states of thought, feeling and experience that constitute memories. Writing a signature, which is never twice identical but is so easily recognized that it is widely accepted as legal tender, provides a classic example. Brain states that support memory recall can also be inferred from direct measurements of neural activity patterns, which are recorded while individuals perform repetitious behaviors. These neural patterns are measured by use of sensors for electric fields (the electroencephalogram, EEG) (Barlow, 1993) magnetic fields (the magnetoencephalogram, MEG), and cerebral blood flows as indirect indicators of metabolism supporting neural activity, for example, functional magnetic resonance imaging (fMRI) (Buxton, 2001), blood oxygen level depletion (BOLD), and optical imaging (Arieli *et al.*, 1996; Arieli and Grinvald, 2002).

The present report emerged from detailed studies that were devoted to documenting the states of the olfactory, visual, auditory and somatosensory systems, as they were revealed by their EEGs (Freeman, 2000a; Freeman, Gaál, and Jörsten, 2003). An array of closely spaced electrodes (8×8 with 0.5 to 0.8 mm spacing giving windows of 4×4 to 6×6 mm) was surgically fixed on a sensory area of rabbit or cat. After recovery the set of channels showed continual background EEG activity having spatially coherent waveforms over the entire array. The main findings were as follows. In the beta and gamma range (20–80 Hz in rabbits, 35–60 Hz in cats) there were bursts of aperiodic oscillation at continually varying frequencies, which gave spectra of the EEG having the form of $1/f^{\alpha}$, where $\alpha=2\pm1$ and log power decreased linearly with approximately the log frequency squared (Freeman *et al.*, 2003). The bursts recurred at rates in the theta range (2–7 Hz) and alpha range (7–12 Hz), often accompanied by a visible wave in the EEG at the corresponding frequency. The same waveform on all electrodes within the same structure of recording had differing spatial patterns of phase modulation (PM) and amplitude modulation (AM) (Freeman and Viana Di Prisco, 1986; Barrie, Freeman, and Lenhart, 1996).

The temporal waveform and peak frequency of the EEG segments had no relation to stimuli. The spatial AM pattern changed significantly after reinforcement learning by the animals to respond to conditioned stimuli (CSs) in the sensory modality to which the stimuli were directed (Barrie, Freeman, and Lenhart, 1996; Freeman, Gaál, and Jörsten, 2003). Changes in AM pattern were progressive over both serial and discriminative conditioning (Freeman and Viana Di Prisco, 1986). Whenever the subjects were trained to respond to a new CS, a new AM pattern formed with learning. When a previous CS was reintroduced after conditioning to intervening CSs, the AM pattern changed to a new form and did not return to the pre-existing form. When the significance of an odorant pair was exchanged by reversing the contingency of reinforcement, all pre-existing AM patterns changed slightly but significantly. These tests showed that the AM patterns lacked invariance with respect to CSs. They showed that each time a subject identified and classified a CS, whether visual, auditory, somatosensory or olfactory, the sensory cortex created an activity pattern corresponding to the category of the stimulus (Ohl, Scheich, and Freeman, 2001). Each AM pattern construction was guided by a chaotic attractor, which in turn was shaped by synaptic changes in the cortical area that sustained the learning.

Each spatial AM pattern was accompanied by its unique, radially symmetric pattern of phase modulation (PM) defined with respect to the phase of the ensemble average, and at the frequency with maximal power in the spectrum of the AM pattern window (Freeman and Baird, 1987; Freeman and Barrie, 2000; Freeman, 2003). The spatial PM pattern had the form of a cone. The sign and the location of the apex of the phase cone varied randomly from each AM pattern to the next. The gradient (wave number) in rad/m, when converted to m/s by dividing by the temporal frequency in rad/s, fell within the range of the conduction velocities of axons running parallel to the cortical surface. Each step to a new phase cone was accompanied by an apparent discontinuity in the time derivative of the analytic phase (Freeman and Rogers, 2002).

This distinctive jump in phase from one phase cone to another suggested that the formation of an AM pattern required an abrupt and irreversible change in system dynamics. That change was similar to a subcritical Hopf bifurcation and to a step in a trajectory of chaotic itinerancy, because it had the appearance of a temporal discontinuity revealed in the EEG. The temporal resolution of phase was substantially increased by use of the Hilbert transform to define and measure the analytic phase of the EEG on each channel. The phase jumps occurred within the digitizing step. Therefore, the apparent discontinuity was adopted as the sign of a state transition in cortical dynamics, whether or not a phase cone could be discerned.

The objective of this study was to use noninvasive methods of scalp EEG recording in order to search for evidence in normal humans of chaotic itinerancy in the form of phase jumps that involved large areas of the cerebral hemispheres. It turned out that the jumps in phase were most clearly seen by use of the cross correlation between the phase jumps treated as a time series and the unfiltered EEG (Freeman and Rogers, 2002; Freeman, Burke, and Holmes, 2003). Standard clinical equipment was used; other researchers may easily replicate the data. Detailed experimental results presented in a 5-part tutorial (Freeman, 2003a, b; Freeman and Burke, 2003; Freeman, Gaál, and Jörsten, 2003; Freeman and Rogers, 2003) showed that recent developments in brain theory are essential for making sense of the data, particularly a framework containing the concepts of chaotic itinerancy, the state transition, anomalous dispersion, and self-organized criticality.

II. METHODS

The data were collected in the EEG Clinic of Harborview Hospital, University of Washington, Seattle, and sent by ftp without identifying markers or personal information to the University of California at Berkeley. Data collection was governed by protocols in accord with the Helsinki Declaration and approved by the Institutional Review Boards in both

institutions. Nine adult volunteers were asked to sit quietly and relax with eyes closed, and then to open their eyes, or to induce a moderate level of electromyographic activity (EMG) by tensing their scalp muscles without moving (Freeman *et al.*, 2003). A curvilinear electrode array with 64 gold-plated needles at 3 mm intervals for a length of 18.9 cm was fixed on the scalp paracentrally along the part line. Recordings were referential to the vertex or to the contralateral mastoid. EEGs were amplified with a Nicolet [BMSI 5000] system having a fixed gain of 1628 and analog filters set at 0.5 Hz high pass and 120 Hz low pass. The ADC gave 12 bits with the least significant bit of 0.9 microvolts and a maximal range 4096 bits. The digitizing rate was 200 samples/s (5 ms interval), while the analog filter was set at 120 Hz, leaving the possibility of aliasing between 80–100 Hz. Temporal power spectral densities (PSD_t) were calculated with the one-dimensional FFT for every channel after applying a Hanning window to nonoverlapping epochs of 1200 ms, losing 100 ms at each end. The 64 temporal PSD_t were averaged and transformed for display in log–log coordinates. Temporal filters were FIR estimated using Parks–McClellan algorithm of order 200. The transition bandwidth was 4 Hz. Spatial filtering was done in the frequency domain by taking the FFT to get the spatial power spectral density (PSD_x), multiplying by an exponential high and low pass filter (Gonzalez and Wintz, 1977), and taking the inverse FFT of the filtered data (Freeman and Baird, 1987; Barrie, Freeman, and Lenhart, 1996; Freeman *et al.*, 2003).

The analytic phase was defined as the arc tangent of the ratio of the imaginary and real components of the Hilbert transform (Freeman and Rogers, 2002; Freeman, Burke, and Holmes, 2003). The arc tangent was calculated using the inverse tangent function atan. The resulting time series resembled a sawtooth, with small increments along a diagonal from the lower bound to the upper bound, $-\pi$ to $+\pi$, and an immediate single downward fall to the lower bound on reaching the upper bound. In order to track the phase over arbitrarily long time intervals the disjoint phase sequences were straightened. In this study each new phase sequence was triggered when the phase dropped from positive to negative, and π radians were added.

Empirical observations on the relation between the analytic amplitude and the analytic phase indicated that a rapid change in phase tended to occur at a minimum in amplitude. Display of this relation was facilitated by converting the amplitude, AA, to a weighting coefficient,

$$W = 10\exp(-AA/10). \tag{1}$$

The values of W ranged from near zero for high AA to 1 for zero AA. The weight was applied to the absolute value of the difference between the phase value at the time of AA in Eq. (1) and the phase at the preceding step. This improved the detection of spatial synchrony of jumps in phase. Additional experimental details are to be found in the original reports on which this review has been based (Freeman *et al.*, 2003, in press; Freeman, Burke, and Holmes, 2003, submitted).

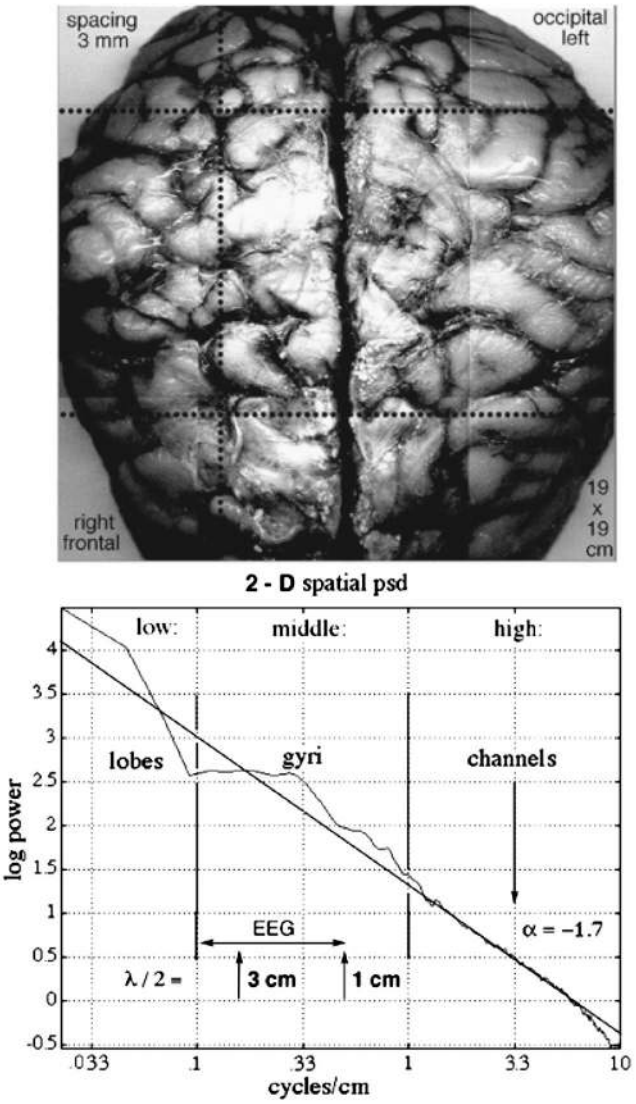

FIG. 1. Upper frame: A montage of photographs shows the surface of a human brain specimen from a teaching collection. The light areas are gyri, and the dark lines are sulci. The scale has been expanded from the radius of the brain, 7.5 cm, to the radius of the scalp, 9.0 cm. The rows of dots show three locations of the 64×1 array of scalp electrodes. Lower frame: The two-dimensional Fourier transform was taken at 1 mm digitizing steps of the photograph for PSD_x in c/cm (wave number in rad/m* $100/2\pi$). The local peak corresponds to the typical length (3 cm) and width (1 cm) of gyri, and to a small peak in the PSD_x of the EEG. From Freeman *et al.* (2003).

III. RESULTS

A. Spatial and temporal spectral properties of scalp EEGs

A montage was constructed of photographs of a normal brain viewed perpendicularly to the curved surface [Fig. 1(A)]. The radius of the brain was 7.5 cm, and the estimated thickness of the skull and scalp was 1.5 cm. The gyri appeared as light areas, and the outer aspects of the sulci appeared as dark curves, indicating the indentations in the wrinkled surface of the cortex. The circumference of the scalp of the nine subjects varied between 56 and 59 cm, giving an approximate radius of 9 cm for the head. The surface view of the cortex was up-scaled to the area of the scalp.

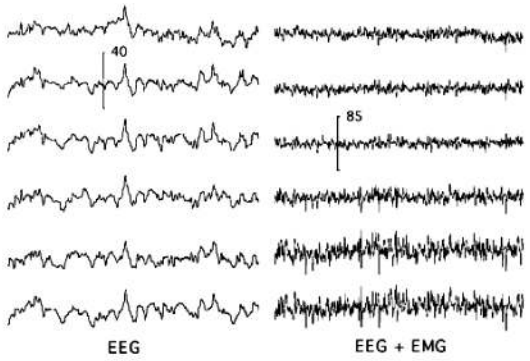

FIG. 2. Examples are shown of the EEG from six consecutive electrodes from a subject with eyes closed and at rest (left), and then during tensing the scalp muscles (right). The amplitude calibration is in microvolts; signal duration is 1 s.

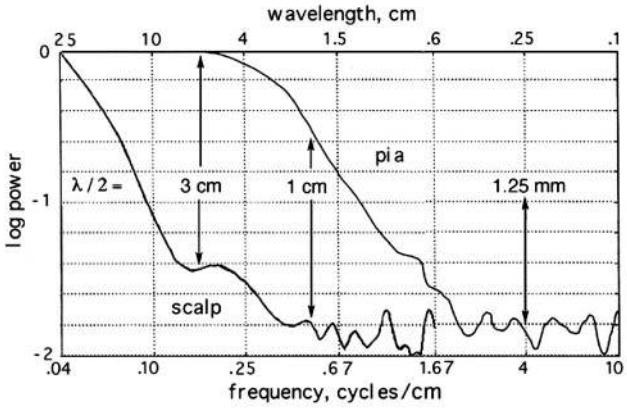

FIG. 3. The one-dimensional spatial PSD_x of human EEG is shown by examples from the scalp (left curve) with electrode spacing of 3 mm and the surface of the superior temporal gyrus of a neurosurgical patient (right curve) with electrode spacing of 0.5 mm. The half-wave length, λ/2, corresponds to the prevailing current Nyquist sampling interval for recording scalp EEG (3 cm), the desired interval proposed here for scalp EEG (1 cm), and the optimal interval for intracranial recording on the pial surface (1.25 mm, Freeman *et al.*, 2000). The pial EEG has the $1/f^{\alpha}$ form, but the scalp EEG does not. From Freeman *et al.* (2003).

The montage was digitized at a grain of 0.1 cm, and the two-dimensional FFT was used to calculate the spatial spectrum of the cortical surface [Fig. 1(B)]. The basic form of the spatial spectrum was $1/f^{\alpha}$, where $\alpha = -1.7$, with a broad peak in the range of 0.1 to 0.5 c/cm, corresponding to the typical width (1 cm) and length (3–5 cm) of human gyri. Superposed rows of dots on the photographic montage indicated the length, spacing, and the three locations of the curvilinear array of recording electrodes. The EEG signals from the array (Fig. 2) were taken with the subject at rest (A) and then while maintaining deliberate muscle tension (B) to contribute electromyographic potentials (EMG).

Prior studies of the spatial spectra from intracranial recording of EEGs in both animals (Freeman and Baird, 1987; Barrie, Freeman, and Lenhart, 1996) and humans (Freeman *et al.*, 2000) had yielded spatial power spectral densities (PSD_x) with the $1/f^{\alpha}$ form (Fig. 3, right curve) with $\alpha = -1.97 \pm 0$. The PSD_x from scalp EEGs (left curve) deviated from $1/f^{\alpha}$ in two ways. First, the power fell more rapidly with increasing spatial frequency, owing to the smoothing done by the high impedance of the skull and scalp intervening between the cortical dendritic current generators and the electrode array. Second, a small peak often appeared in the range of 0.1 to 0.5 c/cm [Fig. 4(A)], corresponding to the texture of the gyri (Fig. 1). When the EEGs were oscillating in phase with nearly zero lag, which was often the case, the fields of electric potential over the convexities of the gyri gave relatively low amplitudes, whereas the fields from the edges of gyri facing into sulci summed and gave relatively high amplitudes. The amplitude differences were subtle and not visible by visual inspection of the signals, and the locations of the mid-range peaks varied at random in accordance with the variations in spatial patterns of the gyri and sulci between subjects.

The temporal power spectral densities (PSD_t) of intracranial and scalp EEGs were both $1/f^{\alpha}$ in form, with $\alpha = 1.78 \pm 0.76$ in frontal EEGs ($N = 9$) and $\alpha = 1.19 \pm 0.28$ in occipital EEGs ($N = 9$) (Freeman *et al.*, 2003 submitted),

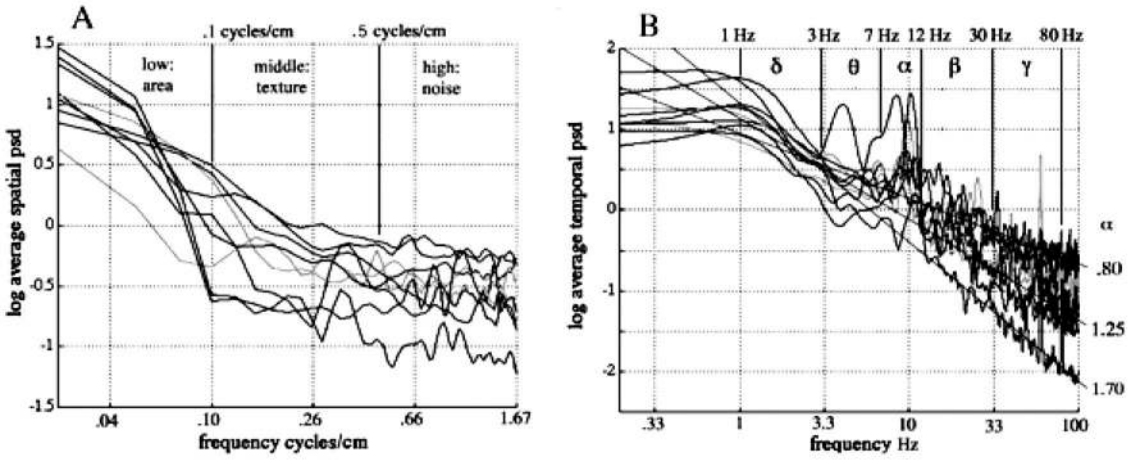

FIG. 4. (A) Examples are shown of the PSD_x of the nine subjects in this study. The three ranges of spatial frequencies correspond to those in Fig. 1. (B) Examples are shown of the temporal PSD_t of the same subjects. The greek letters designate the clinical spectral bands of the EEG. The exponents show the mean slopes of the $1/f^{\alpha}$ form. From Freeman *et al.* (2003).

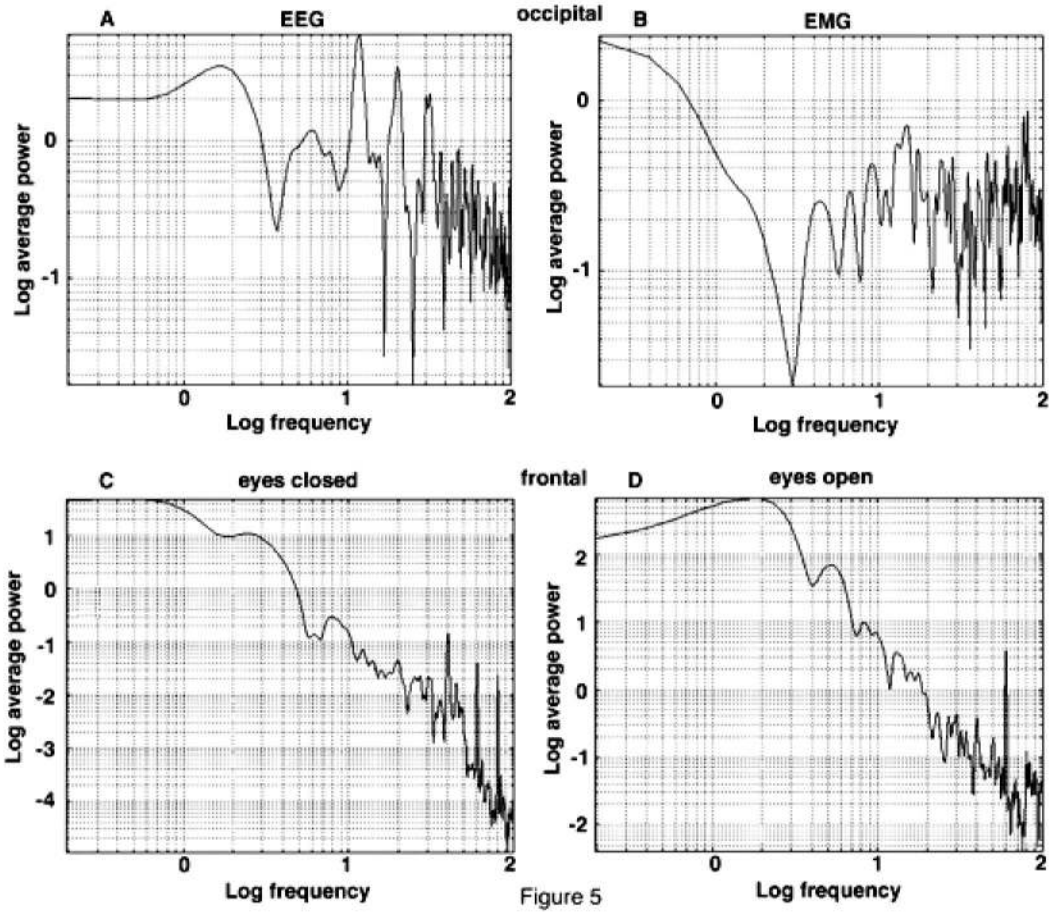

Figure 5

FIG. 5. (A) The temporal PSD$_t$ of the scalp EEG in a subject at rest with eyes closed showed the $1/f^{\alpha}$ scaling with prominent spectral peaks in the alpha and gamma ranges. (B) Upon the induction of EMG the spectral peaks disappeared, and the $1/f^{\alpha}$ form was replaced by a flat spectrum characteristic of white noise. (C) Another subject at rest also showed peaks in the alpha and gamma ranges with $1/f^{\alpha}$ scaling. (D) Upon opening the eyes the peaks were attenuated without change in $1/f^{\alpha}$ scaling.

compared with 2.32 ± 0.27 from intracranial recording (Freeman *et al.*, 2000). In examples taken from the nine subjects at rest with eyes closed [Fig. 4(B)] there were prominent spectral peaks in the alpha range. Occasionally there were also sharp spectral spikes in the gamma range. In contrast to the $1/f^{\alpha}$ scaling of the PSD$_t$ of EEGs [Fig. 5(A)], the PSD$_t$ of EMGs tended to the flat spectrum that characterized wideband noise [Fig. 5(B)], despite the similarities of the time series of the EMG and EEG [Figs. 1(A) and 1(B)]. The alpha peak (7–12 Hz) usually disappeared from the PSD$_t$ on opening the eyes or tensing of scalp muscles, often to be replaced with a peak in the theta range (3–7 Hz), but without loss of the $1/f^{\alpha}$ scaling unless EMG supervened.

B. Studies of the analytic phase and its time derivative

The analytic phase and amplitude were derived by the Hilbert transform using the Cauchy principal value. An essential step before the transform was to band pass filter the EEG on every channel. Studies using behavioral correlation in animals had shown that an optimal pass band could be found by cross correlating the unfiltered EEG with the derivative of the analytic phase (Freeman and Rogers, 2002). Preliminary exploration of the human EEG by this technique gave an optimal pass band of 12–30 Hz, which was in the beta range (Fig. 4). An example of the polar plot of the real and imaginary parts after filtering (Fig. 6) showed the end of the vector starting at the asterisk to the left of the imaginary axis, rotating counterclockwise through the dots, and ending at the asterisk to the right of the imaginary axis. On three occasions in this example the analytic amplitude, given by the length of the vector, closely approached the origin. On these occasions the successive analytic phase differences departed strongly from the mean step size corresponding to the mean frequency in rad/s, either by going negative or by rising to high positive values in radians. Unwrapping of the phase (Fig. 7) replaced the sawtooth curve (black) with a ramp (blue) by adding steps of phase (red staircase).

The temporal numerical differences of the analytic phase were used to approximate the time derivative of the signal from each channel. Experience with intracranial recording in animals (Freeman and Rogers, 2002) had shown that the analytic phase at each location fluctuated over a narrow range in time windows on the order of 80–100 ms. Large spikes in the numerical derivative bracketed these quiet periods. The spikes varied randomly in sign, positive or negative. To sim-

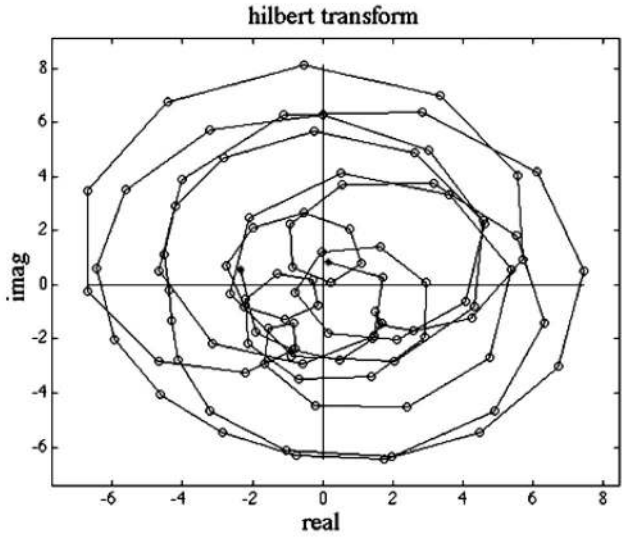

FIG. 6. The Hilbert transform in effect took the temporal derivative of the EEG (the real part) to get the imaginary part (imag) after band-pass filtering (12–40 Hz). The pairs of sequential values in time at the digitizing interval (5 ms) in the complex plane described a vector that rotated counterclockwise. In a representative time segment lasting 500 ms it started at the asterisk to the left of the imaginary axis and ended at the asterisk to the right. The length of the vector gave the analytic, and arc tangent of the ratio, imag/real, gave the analytic phase. Phase jumps occurred most often when the analytic amplitude approached a minimum, whether or not the loop enclosed the origin.

plify the graphic display, the absolute values were plotted in a raster (Fig. 8). The 64 time derivatives plotted as time series showed that the jumps in analytic phase tended to occur almost simultaneously on multiple contiguous channels. Spatial synchrony was revealed by jumps that occurred on lines parallel to the right abscissa labeling the channel locations. Often the jumps occurred over the entire array, simultaneously within the limit of time resolution of the digitizing step (5 ms). To reduce the variance, the phase differences were weighted by Eq. (2) in order to use the additional information provided by the analytic amplitude, on the premise that changes in cortical state occurred at times when

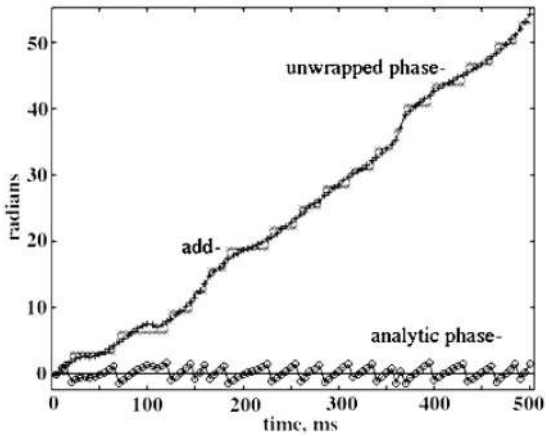

FIG. 7. The time series of the analytic phase appeared in a sawtooth form limited by $\pm\pi$. An unwrapping gave a smooth function by adding π radians at each break point.

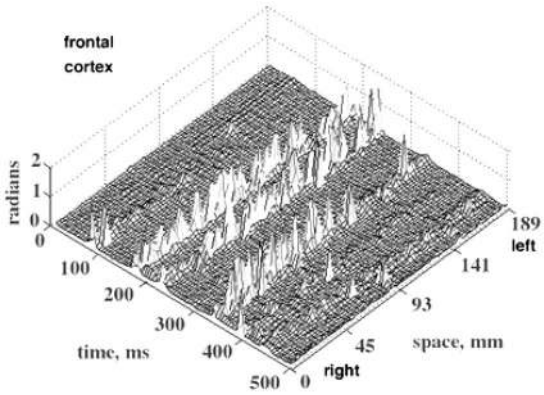

FIG. 8. The temporal numerical differences approximated the time derivative of the analytic phase on lines parallel to the left abscissa at 5 ms intervals. The data were the 64 EEGs from the curvilinear array placed over the frontal lobes across the midline. The channels were spaced at 3 mm intervals as shown on the right abscissa. The plateaus indicated stability of phase. The spikes were the jumps in rate of change in phase. For display the absolute values of the differences were weighted by Eq. (2). The temporal pass band was optimized at 12–30 Hz by maximizing the cross correlation of the signed derivative with the raw EEG in the alpha range of the spectrum. Spatial synchrony was indicated by alignment of the jumps in phase parallel to the right abscissa. A traveling wave would have appeared along a diagonal line. This parallel alignment was independent of the orientation of the array on the scalp.

a minimum of analytic amplitude occurred with a maximal rate of analytic phase change. The spatial synchrony could not be attributed to referential recording, because an event occurring at the reference electrode would appear to be the same on all channels, whereas the sign of the jump varied randomly across the channels.

The plateaus and jumps in the analytic phase were usually restricted to portions of the array (Fig. 9). In this example, the array was placed across the midline over the occipital lobes [the upper row of dots in Fig. 1(A)]. The regions of synchrony extended over both right and left hemispheres but were asynchronous bilaterally. A low pass spatial filter was set at 0.5 c/cm to remove high spatial frequency channel noise (Figs. 1 and 4). The setting of the lower limit of the temporal pass band in all subjects was optimally at the upper limit of the alpha band, 12 Hz. Changes in the setting of the upper limit gave different patterns in different subjects and conditions [Figs. 9(B)–9(D)]. The cross correlation was calculated between the unfiltered EEG and the derivative of the analytic phase after filtering. This function peaked in the alpha or theta range in most subjects. A maximal value occurred when the upper cutoff was at 30 Hz [Fig. 9(B)]. When higher settings were used, a greater density of phase jumps appeared [(C) and (D)], and the correlation decreased.

An example from another subject [Fig. 10(A)] also showed the EEG recorded from an array placed parallel to the midline over the right frontal and parietal lobes. The region of synchrony of the jumps in analytic phase appeared to straddle the central sulcus, although MRI was not used to verify this anatomical relationship. When the subject induced EMG [Fig. 10(B)], the location of the region of synchrony shifted, and the mean repetition rate dropped from the alpha range into the theta range [Figs. 5(A)–5(B)]. This shift from alpha to theta also took place when the subject complied

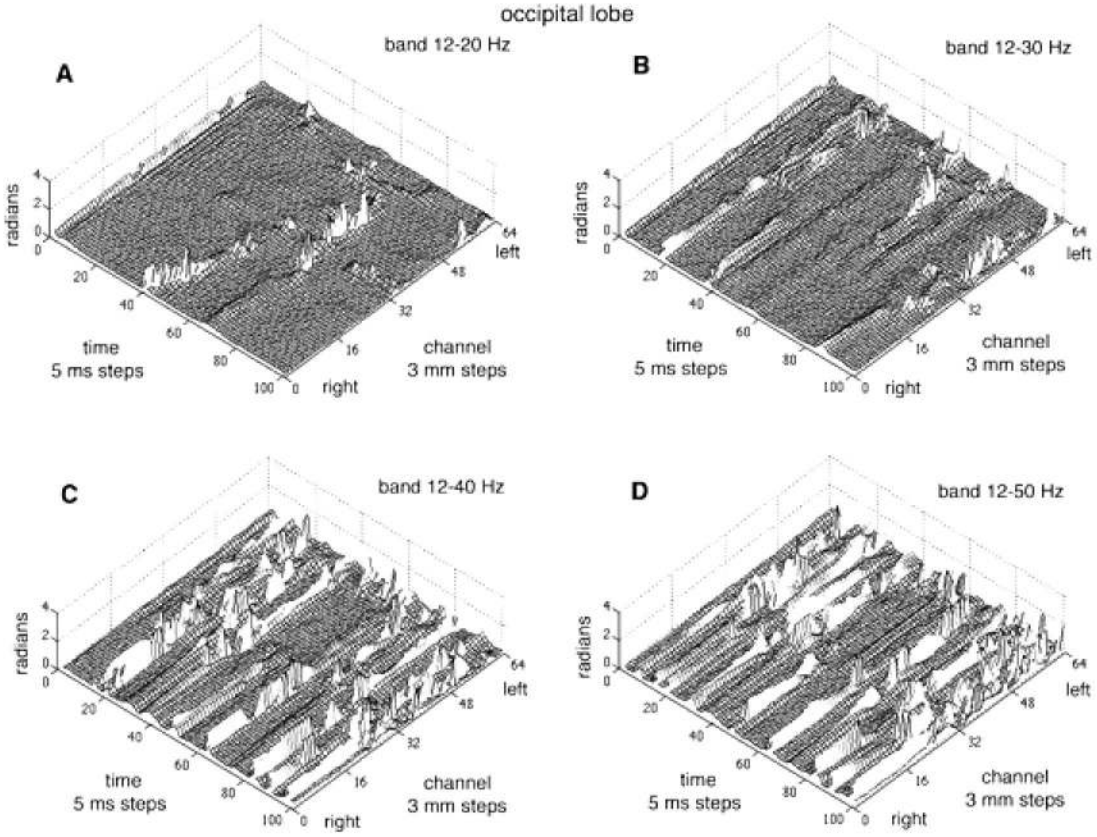

FIG. 9. The effects are shown of varying the upper cutoff of the temporal pass band. Low pass spatial filtering to remove channel noise as defined in Fig. 1 smoothed the data. The recording across the occipital midline revealed the asynchrony between the hemispheres.

with the request to open the eyes [Figs. 5(C)–5(D)]. At rest a spectral spike often appeared [Fig. 5(C)] in the gamma range (30–50 Hz), particularly in the vicinity of 40 Hz (not to be confused with 60 Hz), and this also tended to vanish when the subjects opened the eyes [Fig. 5(D)].

IV. DISCUSSION

The temporal derivative of the analytic phase revealed broad spatial synchrony of the discontinuities in the analytic phase. This synchrony came to light owing to five technical advances. First, the use of the Hilbert transform was essential to provide the required degree of temporal resolution. Second, the application of the transform was made possible by the design of temporal band pass filters that were parametrized by first correlating the raw EEG with the time derivative of the analytic phase after filtering, and then repeating while varying the filter settings in order to maximize the correlation of phase jumps with the alpha activity as the criterion for optimality. Third, the spatial resolution of the EEG was increased by use of a high-density curvilinear electrode array. Fourth was reliance on human subjects, because few animals have brains of such enormous size. Fifth, scalp recording was necessary, because the required extent of surgical exposure of the brain would be too great to be permissible for intracranial recording. The necessity for the conjunction of these advances explains why this phenomenon has not previously been observed.

Temporal and spatial patterns of phase with high resolution were first observed and measured in EEGs by intracranial recording in animals with two-dimensional electrode arrays (8×8 electrodes spaced 0.5 mm giving a 6×6 mm window) placed surgically over the cortical surface. The 64 values of phase were measured by means of the Fourier transform (Freeman and Barrie, 2000) in a moving time window of 64–256 ms at the frequency with the most power. The phase values were found to form stable spatial patterns that lasted 80–100 ms and that emerged repeatedly at rates of 2–7 Hz. The spatial phase gradients in these patterns were measured in rad/mm by fitting a plane or a cone to the 64 phase values. When converted to m/s by use of the frequency at which the phase values were defined, the gradients were equivalent to the conduction velocities of axons running parallel to the cortical surface. The temporal discontinuities at the onsets of the spatial patterns of phase were detected by use of the Hilbert transform (Freeman and Rogers, 2002). The jumps in analytic phase were almost but not quite simultaneous across the array. They were spread over 4–8 ms, which was consistent with the conduction delay observed with the Fourier method. The range of that distribution was also equivalent to the limiting conduction velocity for cortical events that was imposed by the necessity for communication among cortical neurons by propagating action potentials, comparable to what physicists call an event horizon.

Histograms of the intervals between phase jumps by the

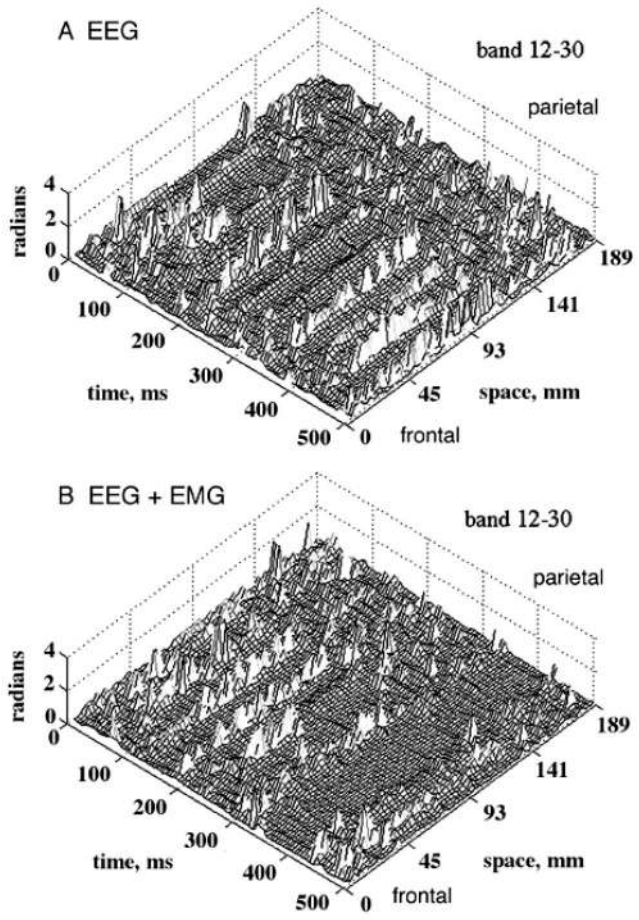

FIG. 10. The recording was made with the curvilinear array placed parallel to the midline over the right frontal and parietal lobes (the vertical row of dots in Fig. 1, upper frame). (A) A record from another subject at rest showed the temporal synchrony of the jumps in the analytic phase across the middle part of the curvilinear array. (B) The alignment persisted into induction of EMG by intentional action but at a lower recurrence rate.

Hilbert transform showed exponential distributions, with highest number of occurrences for the shortest segments, which were at the limit determined by the digitizing rate (here 500/s, Freeman and Rogers, 2002). Histograms of the durations and sizes of the spatial patterns of phase showed that the greatest number of segments having stable phase patterns by the Fourier transform also had the shortest durations and smallest diameters. The exponential decrease in number of segments with increasing duration or interval indicated that these distributions were fractal. However, only the largest and longest lasting of the phase patterns in these distributions were related to behavior through the classification of the AM patterns with respect to conditioned stimuli (Freeman and Barrie, 2000). These large patterns are established by the long, fast axons in cortex, which select the attractors that govern their creation.

The exponential distributions and the $1/f^{\alpha}$ form of the temporal and spatial spectra demonstrated the spatio-temporal scaling properties manifested in EEG (Ingber, 1995; Barrie, Freeman, and Lenhart, 1996; Nunez, 1981; Linkenkaer-Hansen *et al.*, 2001; Freeman *et al.*, 2000; Hwa and Ferree, 2002). The EEG data from animals and humans together showed that spatially coherent cortical activity patterns could coexist in each cerebral hemisphere for epochs ranging in duration from ms to s, over spatial patches that ranged in diameter from under a mm to an entire hemisphere, cascading from hypercolumns through Brodmann's areas, gyri and lobes. The implication was that while most of the adaptive steps were small, brief and numerous, some lasted long enough and were large enough to manifest the salient steps by which the brains adapted to important features of the environment, such as the arrival of an expected CS. It was this relatively small fraction of the phase transitions and AM patterns that was selected by the observers using correlation of the EEG with behavior. And it was the small fraction of large-scale phase transitions that was manifested in the synchronous jumps over wide extents of the scalp EEG, as reported in this review.

These statistical properties characterize a system that can maintain itself in a state of self-organized criticality (Bak, Tang, and Wiesenfeld, 1987; Bak, 1996). The brain can be regarded as a massively interactive organ that maintains itself in a metastable state that combines long-term continuity with the capacity for rapid change in accord with sudden and unpredictable changes in its environments both inside and outside the body. The jumps observed in the derivative of the analytic phase of the scalp occurred at widely distant locations virtually simultaneously in time intervals as brief as the digitizing interval of 5. In many instances the apparent time required for the jump at each location was under one digitizing step, and the jumps were sometimes seen at all 64 electrodes covering a distance of nearly 20 cm in 5 ms, irrespective of the orientation of the curvilinear array on the scalp. The indicated conduction velocity was at least 40 m/s, which was much faster than most intracerebral axons, though not as fast as the fastest peripheral axons (100 m/s).

The oscillation at each location was a standing wave. This condition was demonstrated by recording the phase relations between the excitatory and inhibitory neurons in each location and showing the predicted quarter cycle phase lag of the inhibitory neurons from the excitatory neurons that was predicted for a negative feedback loop (Freeman, 1975). The illusion of traveling waves over the cortical surfaces on impulse input was due to the finite conduction velocity of the axons carrying the input. An analogous relationship would be the appearance of a wave in a field of grain caused by the wind over the field and not by the interactions of the stalks of wheat. This condition was essential to maintain the AM patterns and minimize local smearing. Certainly the medium was interactive, but the radial distances and rates of conduction of interaction were too small to account for global synchronization.

The apparent incompatibility of nearly zero-lag synchrony with axonal conduction delays (Freeman, 2000b) is consistent with recent results from modeling (Chapman, Bourke, and Wright, 2002). It might be consistent with an analogy from optics, where a distinction is made between group velocity and phase velocity in media that conduct light. The transmission speed of energy and information in all media can never exceed the speed of light, but when the frequency of the carrier light is close to an absorption or

resonance band of a medium, the group velocity can differ from the phase velocity (Hecht and Zajac, 1974, pp. 42 and 205). Then light at the group velocity manifests anomalous dispersion. The group velocity might correspond to the average rate of serial synaptic excitation and inhibition across extensive areas of neuropil. This process is dense but is relatively slow, because most axons are under 1 mm in length, and many serial synapses would be required for spread over several cm. Yet axosynaptic transmission is the main basis for cortical exchanges of information. The phase velocity might correspond to the spatial rate of spread of a state transition across the cortex, which as explained below is unlikely to carry significantly dense textures of information. The phenomenon of rate of spread of state change that exceeded serial synaptic transmission and resembling anomalous dispersion was first discovered in the olfactory bulb (Freeman, 1990). Analysis of phase measurements in the bulbar EEG showed that the direction and velocity of propagation of the phase transition could not be explained by the properties of the incoming afferent axons, and that it exceeded the velocity of serial synaptic transmission across the bulb by a factor of about 20. This meant that the entire bulb transitioned from one state to another in about 5 ms instead of the 100 ms required for serial spread (Freeman, 1975). That high rate of change kept the distribution of phase differences within the bulb under a quarter cycle of the gamma carrier frequency (Freeman, 1990). The minimization of phase dispersion is necessary for read-out of bulbar AM patterns, because the divergent-convergent projection of the axons carrying the output enacts a spatial integral transform on the output. Phase dispersion $< \pi/4$ radians leads progressively to loss of detail.

The spread of a state transition at a high velocity resembling the phenomenon of anomalous dispersion in bulb and neocortex could trigger the expression of information previously stored in the attractors of cortical landscapes. That information would emerge in spatial AM patterns of beta and gamma oscillations, with acceptable time lags between widely separated areas. A small proportion of long axons would provide the neural mechanism. Although most intracortical axons are under 1 mm in length, a small subset extends over long distances. The long axons can induce small world effects (Watts and Strogatz, 1998), because an area of cortex that is held close to the separatrix of its basin of attraction may be sensitized to cross over in response to a very small perturbation. The trigger may be provided by the long axons. It would likely involve thalamic control (Hoppensteadt and Izhkevich, 1998; Taylor, 1997; Steriade, 2000), but might best be seen as an emergent property endowed by the state of self-organized criticality (Freeman, 2003a). Experimental data show that the entire cerebral cortex is constantly simmering in the fractal distributions of phase transitions that give the $1/f$ form to the spatial and temporal spectra (Freeman, 2003b). The system is continually primed for global transitions at the longer intervals corresponding to the larger size of the areas of coordination. Thus the recurrence rates of the phase transitions may be an intrinsic clock of the neocortex viewed as an integrated tissue maintaining itself at SOC. Subcortical controls may finetune the reset intervals of the clock. The behaviorally related content in AM patterns of the beta and gamma oscillations, up to the entire extent of both cerebral hemispheres, would be locally determined by intracortical synapses, but the attractors by which that content is accessed would be selected globally.

V. CONCLUSIONS

Integrative brain science is an intellectual structure that is emerging at a unique location in the landscape of human knowledge, where neuroscience overlaps with physics, chemistry, and the behavioral sciences. The sine qua non of this structure is the collection of data describing the forms and functions of neurons and their combinations in networks and populations, including the fields of electromagnetic potential and related forms of energy by which neural activity is expressed. However, in order to interpret their data brain scientists have to measure animal and human behavior and relate it to neural activity. In doing this they have to rely on abstract psychological and philosophical concepts such as intention (Freeman, 2000c), attention, motivation, meaning (Barham, 1996; Freeman, 2003a), causation and consciousness. And in order to plan their experiments in electrophysiology brain scientists have to use basic physical concepts such as energy, power, entropy, and information. Now with the growth of theory in complexity and chaos these fundamentals do not suffice to make sense out of vast quantities of new data revealing structure that is unfamiliar and baffling.

New concepts are emerging, first among them being the state transition as elaborated by Haken (1999) in the order parameter and slaving principle that guide the formation of assemblies of particles. The state transitions in distributed media are not simultaneous everywhere but begin at sites of nucleation and spread radially, as in the formation of a raindrop. The analogy of a cortical state transition with a phase transition from vapor to liquid is appealing in terms of the radially symmetric gradients of phase cones and the increase in constraints among particles that is implicit in synchronization of neural oscillations. The analogy fails in other respects, principally that cortex operates far from thermodynamic equilibrium, and there is no defined entity to compare with latent heat. The disjunction between the low rates of serial synaptic transmission and the high phase velocities inferred from conic phase gradients indicates that neural populations have two classes of velocities. Both are consistent with the limits of axon impulse transmission, but the slow velocities reflect information transmission, whereas the high velocities reflect the spread of changes in state without transmission of information but with selection of already stored information. This distinction suggests the analogy with anomalous dispersion. The high velocity of spread of phase transitions can synchronize the oscillations in the beta–gamma range, which in turn express their structure in AM patterns. This is an example where a well-defined concept from physics can provide a scaffold for the experimental exploration of a phenomenon that might otherwise be overlooked or explained away.

The overlap of phase cones in all cortical sites where they are found indicates that state transitions occur continu-

ally in every area of cortex, leading to superimposed spatial patterns of coherent activity with fractal distributions of size and duration. The circumstantial evidence for self-organized criticality is compelling, but the nature of the critical state is still unknown in neurobiological terms. The spatial and temporal PSD of EEGs often show the $1/f^{\alpha}$ form, but more often there is distortion by clinically defined peaks and, in the case of scalp EEG, by muscle potentials (EMG), so measurements of α are unreliable and vary widely without evident behavioral or electrophysiological correlations to give them meaning.

The aperiodic oscillations giving $1/f^{\alpha}$ PSD are commonly referred to as chaotic, but brain activity is not at all consistent with low-dimensional deterministic chaos. It is high dimensional, noisy, non-Gaussian, nonstationary, and nonautonomous, because brains are open systems driven by stochastic input. Alternative names have been proposed for brain activity, such as stochastic chaos (Freeman, 2003c) and nonconvergent dynamics (Principe *et al.*, 2001), because brain activity is based in the random firing of billions of independent neurons that interconnect, interact, and constrain each other in massive populations. That constraint decreases the degrees of freedom of the neurons in ways similar to the effects of band pass filtering, but brain activity is not filtered noise, neither does it conform to the mathematical nor lexical definitions of chaos. Therefore, whether the term chaotic itinerancy is appropriate to describe repetitive state transitions in cortex remains open to challenge. My conclusion is that the term is useful in the interim as a means to engage the interest and active participation of physicists and mathematicians in the study of brain dynamics. As we learn more about it, an appropriate term will emerge by consensus and shared practice. Meanwhile, I hope that physicists will worry less about proving theorems and more about helping to explain complex patterns in spatio-temporal data.

ACKNOWLEDGMENTS

The work underlying this review was funded in part by research grants from NIMH (MH06686), ONR (N63373 N00014-93-1-0938), NASA (NCC 2-1244), and NSF (EIA-0130352). EEG and EMG data were collected and edited by Dr. Mark D. Holmes and Dr. Sampsa Vanhatalo in the EEG Clinic of Harborview Hospital, University of Washington, Seattle. The experimental results are presented in full by a 5-part tutorial in the International Journal of Bifurcation Chaos Appl. Sci. Eng.

Arieli, A., and Grinvald, A. (**2002**). "Optical imaging combined with targeted electrical recordings, microstimulation or tracer injections," J. Neurosci. Methods **116**, 15–28.

Arieli, A., Sterkin, A., Grinvald, A., and Aertsen, A. (**1996**). "The dynamics of ongoing activity accounts for the large variability in cortical evoked responses," Science **273**, 1868–1871.

Bak, P. (**1996**). *How Nature Works: The Science of Self-organized Criticality* (Copernicus, New York).

Bak, P., Tang, C., and Wiesenfeld, K. (**1987**). "Self-organized criticality: an explanation of 1/*f* noise," Phys. Rev. Lett. **59**, 381–■■.

Barham, J. (**1996**). "A dynamical model of the meaning of information," BioSystems **38**, 235–241.

Barlow, J. S. (**1993**). *The Electroencephalogram: Its Patterns and Origins* (MIT Press, Cambridge, MA).

Barrie, J. M., Freeman, W. J., and Lenhart, M. D. (**1996**). "Spatiotemporal analysis of prepyriform, visual, auditory and somesthetic surface EEG in trained rabbits," J. Neurophysiol. **76**, 520–539.

Buxton, R. B. (**2001**). *Introduction to Functional Magnetic Resonance Imaging: Principles and Techniques* (Cambridge University Press, New York).

Chapman, C. L., Bourke, P. D., and Wright, J. J. (**2002**). "Spatial eigenmodes and synchronous oscillation: coincidence detection in simulated cerebral cortex," J. Math. Biol. **45**, 57–78.

Freeman, W. J. (**1975**). *Mass Action in the Nervous System* (Academic, New York).

Freeman, W. J. (**1990**). "On the problem of anomalous dispersion in chaoto-chaotic phase transitions of neural masses, and its significance for the management of perceptual information in brains," in *Synergetics of Cognition*, edited by H. Haken and M. Stadler (Springer-Verlag, Berlin), Vol. 45, pp. 126–143.

Freeman, W. J. (**2000a**). *Neurodynamics. An Exploration of Mesoscopic Brain Dynamics* (Springer-Verlag, London, UK).

Freeman, W. J. (**2000b**). "Characteristics of the synchronization of brain activity imposed by finite conduction velocities of axons," Int. J. Bifurcation Chaos Appl. Sci. Eng. **10**, 2307–2322.

Freeman, W. J. (**2000c**). "A proposed name for aperiodic brain activity: Stochastic chaos," Neural Networks **13**, 11–13.

Freeman, W. J. (**2003a**). "A neurobiological theory of meaning in perception. Part 1. Information and meaning in nonconvergent and nonlocal brain dynamics," Int. J. Bifurcation Chaos Appl. Sci. Eng. (in press).

Freeman, W. J. (**2003b**). "A neurobiological theory of meaning in perception. Part 2. Spatial patterns of phase in gamma EEG from primary sensory cortices reveal the properties of mesoscopic wave packets," Int. J. Bifurcation Chaos Appl. Sci. Eng. (in press).

Freeman, W. J., and Baird, B. (**1987**). "Relation of olfactory EEG to behavior: Spatial analysis," Behav. Neurosci. **101**, 393–408.

Freeman, W. J., and Barrie, J. M. (**2000**). "Analysis of spatial patterns of phase in neocortical gamma EEG in rabbit," J. Neurophysiol. **84**, 1266–1278.

Freeman, W. J., and Burke, B. C. (**2003**). "A neurobiological theory of meaning in perception. Part 3. Multicortical patterns of amplitude modulation in gamma EEG," Int. J. Bifurcation Chaos Appl. Sci. Eng. (in press).

Freeman, W. J., Burke, B. C., and Holmes, M. D. (**2003**). "Aperiodic phase re-setting in scalp EEG of beta-gamma oscillations by state transitions at alpha-theta rates," Human Brain Mapping (submitted).

Freeman, W. J., Burke, B. C., Holmes, M. D., and Vanhatalo, S. (**2003**). "Spatial spectra of scalp EEG and EMG from awake humans," Clin. Neurophysiol. **114**, 1055–1060.

Freeman, W. J., Gaál, G., and Jörsten, R. (**2003**). "A neurobiological theory of meaning in perception. Part 2. Multiple cortical areas synchronize without loss of local autonomy," Int. J. Bifurcation Chaos Appl. Sci. Eng. (in press).

Freeman, W. J., and Rogers, L. J. (**2002**). "Fine temporal resolution of analytic phase reveals episodic synchronization by state transitions in gamma EEG," J. Neurophysiol. **87**, 937–945.

Freeman, W. J., and Rogers, L. J. (**2003**). "A neurobiological theory of meaning in perception. Part 4. Multicortical patterns of phase modulation in gamma EEG," Int. J. Bifurcation Chaos Appl. Sci. Eng. (in press).

Freeman, W. J., Rogers, L. J., Holmes, M. D., and Silbergeld, D. L. (**2000**). "Spatial spectral analysis of human electrocorticograms including the alpha and gamma bands," J. Neurosci. Methods **95**, 111–121.

Freeman, W. J., and Viana Di Prisco, G. (**1986**). "Relation of olfactory EEG to behavior: Time series analysis," Behav. Neurosci. **100**, 753–763.

Gonzalez, R. C., and Wintz, P. (**1977**). *Digital Image Processing* (Addison-Wesley, Reading, MA).

Haken, H. (**1999**). "What can synergetics contribute to the understanding of brain functioning?" in *Analysis of Neurophysiological Brain Functioning*, edited by C. Uhl (Springer-Verlag, Berlin), pp. 7–40.

Hecht, E., and Zajac, A. (**1974**). *Optics* (Addison-Wesley, Reading, MA), pp. 38–42, 205–205.

Hoppensteadt, F. C., and Izhkevich, E. M. (**1998**). "Thalamo-cortical interactions modeled by weakly connected oscillators: could the brain use FM radio principles?" BioSystems **48**, 85–94.

Hwa, R. C., and Ferree, T. (**2002**). "Scaling properties of fluctuations in the human electroencephalogram," Phys. Rev. E **66**, 021901.

Ingber, L. (**1995**). ''Statistical mechanics of multiple scales of neocortical interactions,'' in *Neocortical Dynamics and Human EEG Rhythms*, edited by P. L. Nunez (Oxford U.P., New York), pp. 628–681.

Linkenkaer-Hansen, K., Nikouline, V. M., Palva, J. M., and Iimoniemi, R. J. (**2001**). ''Long-range temporal correlations and scaling behavior in human brain oscillations,'' J. Neurosci. **15**, 1370–1377.

Nunez, P. L. (**1981**). *Electric Fields of the Brain: The Neurophysics of EEG* (Oxford U. P., New York).

Ohl, F. W., Scheich, H., and Freeman, W. J. (**2001**). ''Change in pattern of ongoing cortical activity with auditory category learning,'' Nature (London) **412**, 733–736.

Principe, J. C., Tavares, V. G., Harris, J. G., and Freeman, W. J. (**2001**). ''Design and implementation of a biologically realistic olfactory cortex in analog VLSI,'' Proc. IEEE **89**, 1030–1051.

Steriade, M. (**2000**). ''Corticothalamic resonance, states of vigilance, and mentation,'' Neuroscience **101**, 243–276.

Taylor, J. G. (**1997**). ''Neural networks for consciousness,'' Neural Networks **10**, 1207–1225.

Tsuda, I. (**2001**). ''Toward an interpretation of dynamics neural activity in terms of chaotic dynamical systems,'' Behav. Brain Sci. **24**, 793–847.

Watts, D. J., and Strogatz, S. H. (**1998**). ''Collective dynamics of 'small world' networks,'' Nature (London) **394**, 440–442.